



Towards Body Sensor Network Based Gait Abnormality Evaluation for Stroke Survivors

Sen Qiu^{1,2(✉)}, Xiangyang Guo², Hongyu Zhao^{1,2}, Zhelong Wang^{1,2},
Qimeng Li³, and Raffaele Gravina³

¹ Key Laboratory of Intelligent Control and Optimization for Industrial Equipment of Ministry of Education, Dalian University of Technology, Dalian 116024, China

{qiu,zhaohy,wangzl}@dlut.edu.cn

² School of Control Science and Engineering,

Dalian University of Technology, Dalian 116024, China

³ Department of Informatics, Modeling, Electronics and Systems,
University of Calabria, Via P. Bucci, 87036 Rende, CS, Italy

Abstract. Due to the technological advances of micro-electro-mechanical sensor and wireless sensor network, gait analysis has been widely adopted as an significant indicator of mobility impairment for stroke survivors. This paper aims to propose an wearable computing based gait impairment evaluation method with distribute inertial sensor unit (IMU) mounted on human lower limbs. Temporal-spacial gait metrics were evaluated on more than twenty post stroke patients and ten healthy control subjects in the 10-meters-walk-test. Experimental results shown that significant differences exist between stroke patients and healthy subject in terms of various gait metrics. The extracted gait metrics are consistent with clinical observations, and the position estimation accuracy has been validated by optical device. The proposed method has the potential to serve as an objective and cost-efficient tool for rehabilitation-assisting therapy for post stroke survivors in clinical practice.

Keywords: Body sensor network · Human gait analysis · Information fusion · Rehabilitation · Micro-electro-mechanical sensor

1 Introduction

As a fundamental human need, people's health needs are constantly increasing with the development of social economy. Especially in the reality of accelerated aging of the population all over the world. One fifth people will be over the age of 60 by 2050 according to the statistics of United Nations. This means that the need for devices with health monitoring and managing functions will continue to grow. The health crisis is likely to become more and more severe, especially

for some chronic diseases. For example, stroke is a leading cause of death all around the world as population ages. Nearly four fifths of stroke survivors are suffering from hemiparesis which tends to severely deteriorate limbs mobility due to muscle weakness and Joint degeneration. Walking dysfunction is one of the main problems in the rehabilitation of stroke patients. A typical symptom manifest as gait disorder, characterized by asymmetry between dual feet, insufficient foot elevation, deviant gait phase distribution and reduced range of joint motion (ROM) such as ankle joint. Note that ankle joint is an essential clinical concern, i.e., the plantarflexion and dorsiflexion come from ankle joint are used as an evaluation factor by clinic in post stroke rehabilitation programs [1–5]. Gait assessment has thus become a useful tool to study the effect of gait retraining in stroke patients.

Gait is the external manifestation of human body structure and movement, motor regulation system, behavior and mental activity during walking. Any nerve, muscle and joint disease can lead to walking dysfunction [6–9]. Pathological gait refers to the abnormal state of uncoordinated walking. It is actually caused by diseases of the nervous and motor systems of the human body, skewness of the pelvis, trunk lateral flexion and other reasons. Gait analysis system is based on wearable motion capture system, which captures the movement data of lower limbs and then analyzes and evaluates the walking state of people. Traditional optical device based human gait tracking approach and pressure sensor based methods universally suffer from high cost and rigorous requirements of testing setup, hence limited the larger scale application in the field [10,11]. Regardless of the approach, gait parameters derived from wearable inertial sensors have showed significant differences between post stroke patients with walking aids and healthy subjects able to walk normally without auxiliary facilities [12–15].

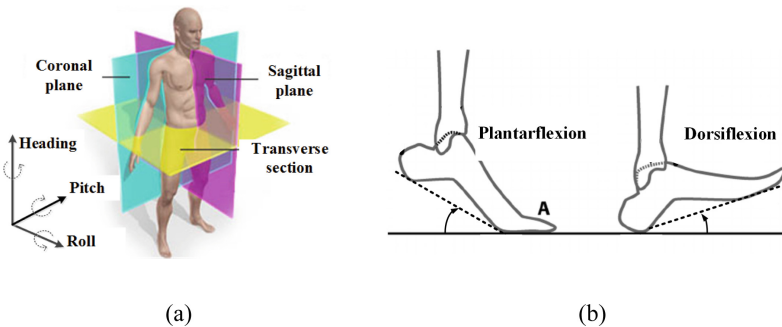


Fig. 1. Three-dimensional anatomical structure and foot movement schematic (a) three planes of the human body (b) foot plantarflexion and dorsiflexion

The three-dimensional anatomical structure is the reference from which all other orientation description are based [16–19], where the subjects' faces are

directed forward, while the toes facing forward, as shown in Fig. 1(a). In this case, three anatomical planes can be defined: the sagittal plane, the transverse plane and the coronal plane, respectively. The coronal plane divides the body into anterior (front) and posterior (rear) sections. The transverse plane divides the body into superior (upper) and inferior (lower) sections. The sagittal plane divides the body into left and right halves. With regards to gait analysis, the majority of movements occur within the sagittal plane. Note that the ankle movement to point the toes is called plantarflexion while the movement to bring the toes closer to the body is called dorsiflexion, as shown in Fig. 1(b).

2 Methodology and Materials

2.1 Hardware Platform Based on Wearable IMU

The self-made sensor module weights less than 20 g, the maximum size is not more than 60 mm. The total power consumption does not exceed 200 mW. The lightweight design of sensor module is for the demand of gait analysis and intended to have minimal effect on natural gait of the subjects. The inertial sensor array specification is shown in Table 1. We have designed a bandage that binds the sensor tightly on lower limbs, avoiding direct contact with the skin and allowing the sensor nodes to be adapted to different types of shoes without compromising the reliability of the sensor installation. In the gait assessment scenario, the subject wear multiple sensor nodes on both lower limbs, and their daily activities will not be affected. Movement data from wearable sensors were recorded when the subjects walked at an preferred speed for 10 m along straight line path. The embedded operating system μ COS is adopted to collect the raw sensor data and transmit the data to the host through 2.4 Ghz wireless communication with the data transmission rate of 100 Hz. In addition to real-time wireless transmission, the system can rely on the memory card for offline recording, which supporting more than 10 h of continuous monitoring. This performance enhances its portability and is very helpful in outdoor testing scenario, where subjects are not restricted to stay in the settled wireless communication coverage area. Figure 2 illustrate the raw motion data of dual foot during normal walking.

Table 1. Inertial sensor array specification

| Unit | Accelerometer | Gyroscope | Magnetometer |
|-------------------|------------------------|---------------------------|--------------------------|
| Dimensions | 3 axes | 3 axes | 3 axes |
| Dynamic scope | $\pm 50 \text{ m/s}^2$ | $\pm 1200^\circ/\text{s}$ | $\pm 750 \text{ mGauss}$ |
| Bandwidth | 30 Hz | 40 Hz | 20 Hz |
| Nonlinearity | 0.2% | 0.1% | 0.25% |
| Axis misalignment | 0.1° | 0.1° | 0.1° |

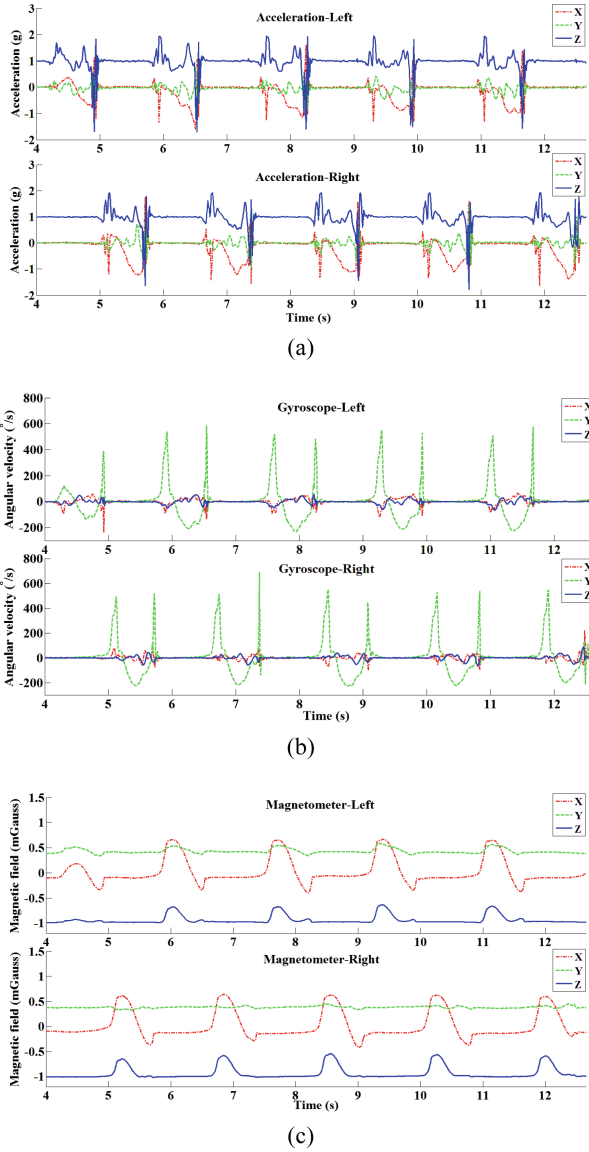


Fig. 2. Raw data collected from IMU (a) Acceleration measurement (b) Gyroscope measurement (c) Magnetometer measurement

The data from the wearable inertial sensors are compared with measurements obtained from an optical motion tracking system. On account of the misalignment error, the accelerometer is accurately calibrated with a linear least squares method. Note that the magnetometer performance is easily distracted by other magnetic source [14, 20–23]. Therefore, it is necessary to estimate the magnetic

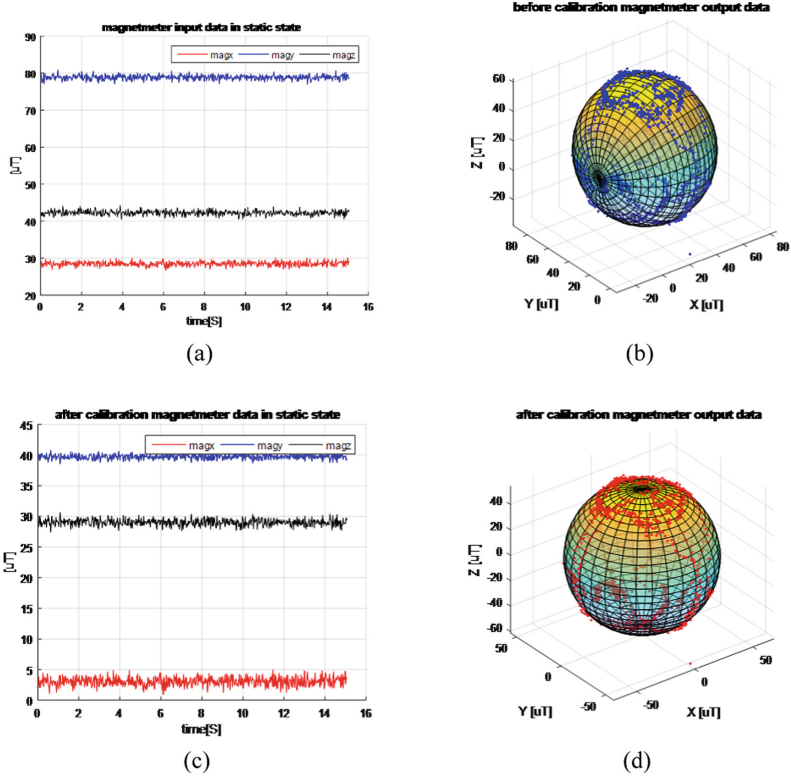


Fig. 3. Fitting results of ellipsoid before and after calibration (a) raw magnetometer measurement (b) ellipsoid fitting before calibration (c) magnetometer measurement after calibration (d) ellipsoid fitting after calibration

interference when using the observation data of the magnetometer to estimate the heading. Set $\mathbf{m}^s = [m_x^s, m_y^s, m_z^s]$ as the measured magnetic field for ground reference, when meet the following criterion, can be directly used magnetic measurement. The threshold λ is set to 0.2 after several tries and errors. Figure 3(a) (b) and (c) (d) are fitting results of ellipsoid before and after calibration respectively. One rotation of the magnetometer is enough to ensure the accuracy of the magnetometer calibration.

$$\left| \frac{\arctan(m_x^s/m_z^s) - \arctan(m_x^g/m_z^g)}{\arctan(m_x^g/m_z^g)} \right| \geq \lambda \quad (1)$$

2.2 Gait Metrics Definition

Gait metrics definition are described in Table 2. The statistics of gait metrics may varied greatly between normal and pathological status. For example, under normal circumstances, the swing phase accounts for 40% of a gait cycle, and the

stance phase takes the remaining 60% [24–27]. For stroke patients, in order to alleviate the pain caused by dystonia, they tend to adopt a relatively comfortable posture, which leads to the increase of stance phase, along with lower foot elevation and gait asymmetry.

Table 2. Typical spatio-temporal gait metrics

| Gait metrics | Description |
|---------------------|---|
| Stride length (m) | Distance between two consecutive footprint of the same foot |
| Walking speed (m/s) | Stride length divided by walking cycle |
| Stance ratio (s) | The proportion of the stance phase in a single walking cycle |
| Foot elevation (m) | Foot elevation in swing phase, which reflects the muscular strength |
| Gait symmetry | Symmetry of walking motion between left and right side of lower limbs |
| Ankle ROM (°) | Range of ankle flexion during a single stride |

$$q = q_0 + q_1\mathbf{i} + q_2\mathbf{j} + q_3\mathbf{k} \quad (2)$$

This research adopts quaternion to represent rigid body rotation, as illustrated in Eq. 2. Note that the rotation from body frame to reference frame can be represented by a rotation angle α around a phasor axis. It is widely acknowledged that the rotation matrix C can describe a rotation of rigid body as follows:

$$C = \begin{bmatrix} q_0^2 + q_1^2 - q_2^2 - q_3^2 & 2(q_1q_2 + q_0q_3) & 2(q_1q_3 - q_0q_2) \\ 2(q_1q_2 - q_0q_3) & q_0^2 - q_1^2 + q_2^2 - q_3^2 & 2(q_2q_3 + q_0q_1) \\ 2(q_1q_3 + q_0q_2) & 2(q_2q_3 - q_0q_1) & q_0^2 - q_1^2 - q_2^2 + q_3^2 \end{bmatrix} \quad (3)$$

where

$$\psi = -\arctan\left(\frac{2(q_1q_2 - q_0q_3)}{q_0^2 + q_1^2 - q_2^2 - q_3^2}\right) \quad (4)$$

$$\theta = \arcsin(2(q_2q_3 + q_0q_1)) \quad (5)$$

$$\varphi = -\arctan\left(\frac{2(q_1q_3 - q_0q_2)}{q_0^2 - q_1^2 - q_2^2 + q_3^2}\right) \quad (6)$$

The combination of roll angle φ , pitch angle θ and yaw angle ψ determine the three-dimensional orientation, which lay a solid foundation for position estimation.

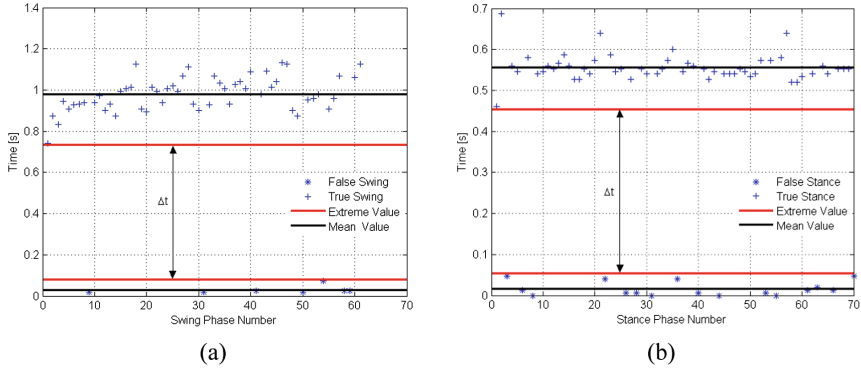


Fig. 4. Gait phase detection by k-mean clustering algorithm (a) swing phases detection (b) stance phases detection

As illustrated in Fig. 4, the k-mean clustering algorithm efficiently classifies the detected swing phases and stance phases into true and false clusters based on time durations, respectively. Meanwhile, the extreme values of each cluster are illustrated by red lines. Results shown that time constraint parameters were determined adaptively for different data sets using the k-mean algorithm, in this case, false gait phases detection due to sensor data fluctuation could be properly eliminated (Fig. 4).

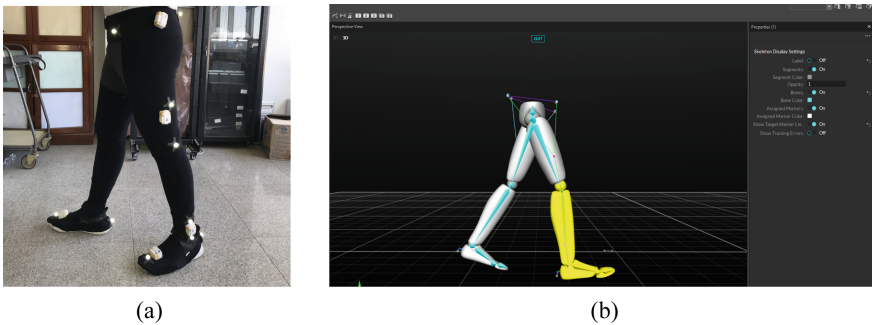


Fig. 5. Experimental scene and optical system validation (a) Inertial sensor installation and high reflection marker for optical motion tracking (b) 3D orientation and position ground truth provided by optical apparatus

2.3 Experimental Results and Discussions

In this research, the subjects included the patients group and the control group. The patients group consists of twenty stroke survivors (ten females and ten

Table 3. Gait parameters comparison for healthy subjects and patients. Results are presented as mean (\pm SD)

| Gait metrics | Healthy subjects | Stroke survivors |
|--------------------------|------------------|------------------|
| Stride length (m) | 1.17 ± 0.15 | 0.72 ± 0.48 |
| Walking speed (m/s) | 0.96 ± 0.15 | 0.64 ± 0.37 |
| Stance ratio (%) | 59 ± 4 | 70 ± 16 |
| Foot elevation (m) | 0.22 ± 0.05 | 0.011 ± 0.09 |
| Gait symmetry | 0.93 ± 0.07 | 0.74 ± 0.26 |
| Ankle ROM ($^{\circ}$) | 66 ± 9 | 39 ± 18 |

Table 4. 3D position estimation error

| Position error | X-axis (m) | Y-axis (m) | Z-axis (m) |
|----------------|-------------------|-------------------|-------------------|
| Trial 1 | 0.017 ± 0.005 | 0.023 ± 0.004 | 0.008 ± 0.003 |
| Trial 2 | 0.014 ± 0.003 | 0.019 ± 0.005 | 0.006 ± 0.004 |

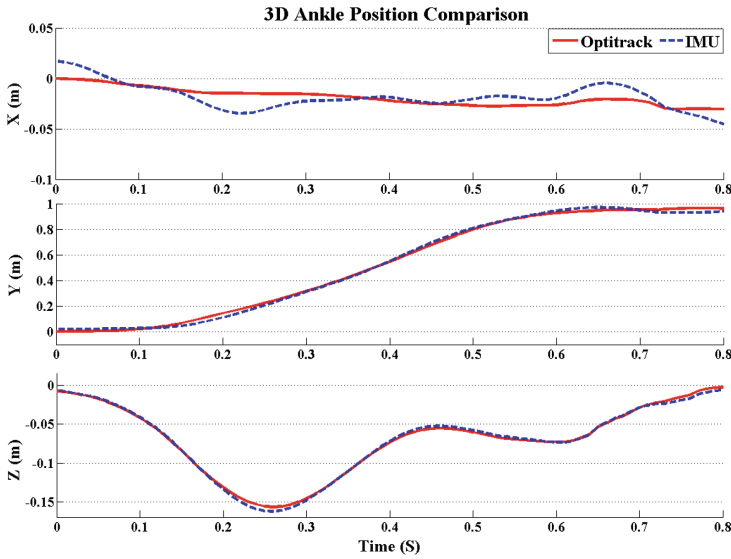


Fig. 6. Results of comparative experiments using Optitrack device

males age from 38 to 67) with varying degrees of gait abnormality. The control group includes ten healthy subjects (five females and five males age from 22 to 46) who participated in the control tests. The tests consist of multiple walking trials along the specific straight line path for each subject at their comfortable pace. The experiment took place in the corridor of first affiliated hospital of Dalian Medical University. The extracted gait metrics are presented in Table 3,

the stride lengths, walking speed, foot elevation, gait symmetry and ankle range of motion (ROM) are relatively low in stroke survivors, which are consistent with clinical observation. The mean value of stride length of healthy subjects are 1.12 ± 0.18 , with the minimum being 0.98 m. The system validation scenario is shown in Fig. 5, and the results of comparative experiments using Optitrack device are shown in Table 4 and Fig. 6.

3 Conclusions

In this work, an IMU based system for ambulatory gait monitoring was presented. The physical interface is connected to the computer by a Bluetooth link, and provides feedback to the medical staff and patients while performing walking trials. The system allows for in-home rehabilitation at an affordable cost.

The essential aspect of wearables sensors in healthcare applications is monitoring the health of users. Body sensors network provides the foundation of numerous medical applications by measuring and processing physiological information upon which medical staff can make intelligent decisions and inform the subjects with quantitative data. Particularly, IMU sensors consist of accelerometers and gyroscopes are readily available on contemporary smartphones and wearable devices. They have been widely adopted in the area of limb movement disorder recognition, fall detection and step counting applications being prominent examples in this field. In the long run, only the combination of hospital, data and equipment can fully reflect the advantages of big data and wearable computing. The battery life, data processing, data collection, transmission and the ability of computers to analyze the data independently are the key to the ultimate solution of gait analysis in the big data era.

Acknowledgments. This research was funded by National Natural Science Foundation of China (61803072, 61873044 and 61903062), China Postdoctoral Science Foundation (2017M621131 and 2017M621132), Liaoning Natural Science Foundation Key Project no. 20180540011, Dalian Science and Technology Innovation fund (2019J13SN99 and 2018J12SN077), Fundamental Research Funds for the Central Universities no. DUT18RC(4)034, and National Defence Pre-research Foundation no. 614250607011708.

References

1. Gravina, R., Alinia, P., Ghasemzadeh, H., Fortino, G.: Multi-sensor fusion in body sensor networks: state-of-the-art and research challenges. *Inf. Fusion* **35**, 68–80 (2016)
2. Fortino, G., Galzarano, S., Gravina, R., Li, W.: A framework for collaborative computing and multi-sensor data fusion in body sensor networks. *Inf. Fusion* **22**, 50–70 (2015)
3. Horak, F.B., King, L., Mancini, M.: Role of body-worn movement monitor technology for balance and gait rehabilitation. *Phys. Ther.* **95**(3), 461–70 (2015)

4. Gravina, R., et al.: Cloud-based activity-aaservice cyber-physical framework for human activity monitoring in mobility. *Future Gener. Comput. Syst.* **75**, 158–171 (2017)
5. Qiu, S., Wang, Z., Zhao, H., Liu, L., Jiang, Y., Li, J.: Body sensor network based robust gait analysis: toward clinical and at home use. *IEEE Sens. J.* **19**, 1–9 (2019)
6. Al-Amri, M., Nicholas, K., Button, K., Sparkes, V., Sheeran, L., Davies, J.L.: Inertial measurement units for clinical movement analysis: reliability and concurrent validity. *Sens. (Switz.)* **18**(3), 1–29 (2018)
7. Kumar, P., Mukherjee, S., Saini, R., Kaushik, P., Roy, P.P., Dogra, D.P.: Multimodal gait recognition with inertial sensor data and video using evolutionary algorithm. *IEEE Trans. Fuzzy Syst.* **27**(5), 956–965 (2019)
8. Qiu, S., Wang, Z., Zhao, H., Liu, L., Jiang, Y.: Using body-worn sensors for preliminary rehabilitation assessment in stroke victims with gait impairment. *IEEE Access* **6**, 31249–31258 (2018)
9. Wang, Q., Markopoulos, P., Yu, B., Chen, W., Timmermans, A.: Interactive wearable systems for upper body rehabilitation: a systematic review. *J. NeuroEngineering Rehabil.* **14**, 1–21 (2017)
10. Baghdadi, A., Cavuoto, L.A., Crassidis, J.L.: Hip and trunk kinematics estimation in gait through Kalman Filter using IMU data at the Ankle. *IEEE Sens. J.* **18**(10), 4253–4260 (2018)
11. Leal-Junior, A.G., Frizera, A., Avellar, L.M., Marques, C., Pontes, M.J.: Polymer optical fiber for in-shoe monitoring of ground reaction forces during the gait. *IEEE Sens. J.* **18**(6), 2362–2368 (2018)
12. Lu, R., Lin, X., Liang, X., Shen, X.: A secure handshake scheme with symptoms-matching for mHealthcare social network. *Mob. Netw. Appl.* **16**(6), 683–694 (2011)
13. Qiu, S., Liu, L., Zhao, H., Wang, Z., Jiang, Y.: MEMS inertial sensors based gait analysis for rehabilitation assessment via multi-sensor fusion. *Micromachines* **9**(9), 442 (2018)
14. Wang, Z., et al.: Using wearable sensors to capture posture of the human lumbar spine in competitive swimming. *IEEE Trans. Hum.-Mach. Syst.* **49**(2), 194–205 (2019)
15. Majumder, S., Mondal, T., Deen, M.J.: A simple, low-cost and efficient gait analyzer for wearable healthcare applications. *IEEE Sens. J.* **19**(6), 2320–2329 (2019)
16. Favre, J., Jolles, B., Siegrist, O., Aminian, K.: Quaternion-based fusion of gyroscopes and accelerometers to improve 3D angle measurement. *Electron. Lett.* **42**(11), 3–4 (2006)
17. Zhao, H., Wang, Z., Qiu, S., Shen, Y., Zhang, L., Tang, K.: Heading drift reduction for foot-mounted inertial navigation system via multi-sensor fusion and dual-gait analysis. *IEEE Sens. J.* **19**(19), 8514–8521 (2019)
18. Gouwanda, D., Gopalai, A.A., Khoo, B.H.: A low cost alternative to monitor human gait temporal parameters-wearable wireless gyroscope. *IEEE Sens. J.* **16**(24), 9029–9035 (2016)
19. Ahmed, M., Naude, J., Birkholtz, F., Glatt, V., Tetsworth, K.: Gait & Posture the relationship between gait and functional outcomes in patients treated with circular external fixation for malunited tibial fractures. *Gait Posture* **68**, 569–574 (2019)
20. Qiu, S., Wang, Z., Zhao, H., Qin, K., Li, Z., Hu, H.: Inertial/magnetic sensors based pedestrian dead reckoning by means of multi-sensor fusion. *Inf. Fusion* **39**, 108–119 (2018)
21. Huang, H., et al.: Attitude estimation fusing quasi-newton and cubature Kalman filtering for inertial navigation system aided with magnetic sensors. *IEEE Access* **6**, 28755–28767 (2018)

22. Gheorghe, M.V., Member, S., Bodea, M.C., Member, L.S.: Calibration optimization study for tilt-compensated compasses. *IEEE Trans. Instrum. Meas.* **67**(6), 1486–1494 (2018)
23. Choe, N., Zhao, H., Qiu, S., So, Y.: A sensor-to-segment calibration method for motion capture system based on low cost MIMU. *Measurement* **131**, 490–500 (2018)
24. Zhao, H., Wang, Z., Qiu, S.: Adaptive gait detection based on foot-mounted inertial sensors and multi-sensor fusion. *Inf. Fusion* **52**, 157–166 (2019)
25. Qiu, S., Wang, Z., Zhao, H., Hu, H.: Using distributed wearable sensors to measure and evaluate human lower limb motions. *IEEE Trans. Instrum. Meas.* **65**(4), 939–950 (2016)
26. Wang, Z., et al.: Inertial sensor-based analysis of equestrian sports between beginner and professional riders under. *IEEE Trans. Instrum. Meas.* **67**(11), 2692–2704 (2018)
27. An, W.W., et al.: Neurophysiological correlates of gait retraining with real-time visual and auditory feedback. *IEEE Trans. Neural Syst. Rehabil. Eng.* **27**(6), 1341–1349 (2019)